

TD–DFT Investigation of Diarylethene Dyes with Cyclopentene, Dihydrothiophene, and Dihydropyrrole Bridges

Eric A. Perpète,^{†,‡} François Maurel,[§] and Denis Jacquemin^{*,†,‡}

Laboratoire de Chimie Théorique Appliquée, Groupe de Chimie Physique Théorique et Structurale, Facultés Universitaires Notre-Dame de la Paix, rue de Bruxelles, 61, B-5000 Namur, Belgium, and Laboratoire Interfaces, Traitements, Organisation et Dynamique des Systèmes (ITODYS), CNRS UMR 7086, Université Paris 7 - Denis Diderot, 1, rue Guy de la Brosse, 75005 Paris, France

Received: February 21, 2007; In Final Form: April 23, 2007

We have investigated the visible spectra of closed-ring diarylethenes presenting cyclopentene, dihydrothiophene, and dihydropyrrole bridging structures. Our simulations have been performed with an ab initio time-dependent density functional theory approach that takes into account bulk environmental effects. The computed λ_{\max} agree qualitatively with experiment, and once a simple statistical treatment is performed, a quantitative agreement is reached. Indeed, after linear fitting correction, the mean absolute error is limited to 6 nm or 0.03 eV for the 57 diarylethenes considered. To unravel the most important parameters for this photochromic class, several structural parameters are correlated to the UV/vis spectra. It turns out that the bond length alternation in the chromogenic unit allows a fast and accurate prediction of the color of these dyes. In addition, we compare our results to available electrochemical data.

I. Introduction

Diarylethene (DA) derivatives, originally described by Irie and Lehn,^{1–5} probably constitute the most well-known and extensively investigated class of thermally stable photochromic molecules.^{6–11} These molecules show both a conjugated closed-ring form and an unconjugated opened-ring form, the direct or reverse conversion being achieved by irradiation at well-separated wavelengths. The two forms have very different electronic (and sometimes magnetic) properties, with, for instance, a colorless open-ring form and a colored closed-ring form. In addition, several DA present exceptionally high fatigue resistance, large quantum yield, and quite small response time, and are therefore serious candidates for optical-storage and photoswitching applications.⁶ The first synthesized DA presented a “bridge” (the moiety keeping attached the two parts of the molecule when in the open form) built with cyano or maleic groups. In 1992, Hanzawa et al. proposed to use perfluoro bridges, and it rapidly appeared that the perfluorocyclopentene DA have many practical advantages.¹² Consequently, most recently designed DA are based upon this structure. Nevertheless, since 2000, Feringa’s group proposed a large panel of cyclopentene DA (**I** in Figure 1).^{13–20} Qin, Yao, and Tian showed in 2003 that such photoswitches can be used for efficiently complexing metal ions.²¹ In this contribution, we predict and rationalize the λ_{\max} of a series of closed-ring cyclopentene DA compounds. In addition, we have considered dihydrothiophene^{22–24} (**II** in Figure 1) and dihydropyrrole^{25–27} (**III** in Figure 1) derivatives that have been synthesized very recently. Our first goal is to predict the color of DA molecules with ab initio calculations, allowing a rapid screening of one

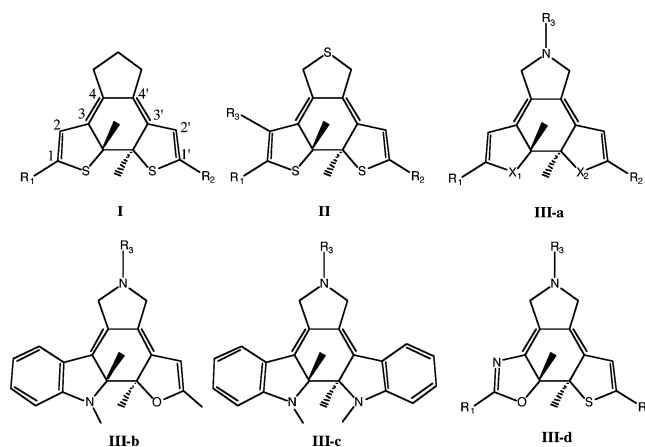


Figure 1. Sketch of diarylethenes investigated.

of the most important property of photoswitches. We also aim to establish structure–property relationships for DA, in order to facilitate the design of new photochroms.

Time-dependent density functional theory (TD–DFT), originally proposed more than two decades ago by Runge and Gross,^{28,29} has become the most widely used tool for theoretically evaluating excited-state energies, and more recently excited-state geometries.^{30–33} This success is due to the TD–DFT efficiency to rapidly provide an accurate description of transition energies. On the contrary, the very accurate ab initio wavefunction approaches EOM-CC, SAC-CI, MR-CI, or CAS-PT2 are in general computationally demanding and difficult to systematically apply on extended sets of molecules, whereas semi-empirical schemes that could be valuable tools to gain chemical insights might reproduce the main experimental trends but definitively lack consistency. For instance, the ZINDO//AM1 approach is much less accurate than TD–DFT for predicting auxochromic displacements in cyano-DA molecules.³⁴ On the contrary, the limitations of TD–DFT (with today’s

* Corresponding author. Electronic address: denis.jacquemin@fundp.ac.be; URL: <http://perso.fundp.ac.be/~jacquemd>.

[†] Research Associate of the Belgian National Fund for Scientific Research.

[‡] Facultés Universitaires Notre-Dame de la Paix.

[§] Université Paris 7 - Denis Diderot.

functionals) are well-understood. Indeed, in the framework of excited-state studies, it tends to leave the tracks when charge separation takes place between distant moieties of the molecule. This is typical for long push–pull oligomers, for which excitation energies are strongly undershot, as nicely rationalized by Tozer.³⁵ Therefore, while the TD–DFT UV/vis spectra tend to agree with experiment for dyes in which the chromophoric unit is well-defined and mainly centered on a few atoms,^{36–38} it might fail for systems like biological complexes³⁹ or cyanine derivatives.^{40,41} In the latter case, CAS-PT2 is required to reproduce the qualitative evolution of the absorption wavelengths when the chain lengthens.⁴² For DA, it is demonstrated in ref 43 that TD–DFT and (the very accurate) SAC-CI results are in good agreement with each other for neutral structures. An important advantage of TD–DFT compared to wavefunction-based approaches is that solvent effects can be included in a straightforward way for both absorption⁴⁴ and emission properties.^{45,46}

Several previous theoretical investigations about diarylethenes focused on determining the reaction path relating the closed and open forms, as the understanding of this intramolecular photoreaction is crucial to maximize the relative stabilities of both structures. These calculations were performed with MNDO or INDO^{47,49} and CASSCF/CAS-PT2,^{50–52} as well as with Hartree-Fock (HF) and DFT.^{14,53–55} It is also worthwhile to point out the simulation of vibrational spectra of de Jong and co-workers.²⁰ For the determination of the electronic transition energies in DA compounds, we are aware of previous studies, possibly using semiempirical approaches,^{56,57} that provide qualitative insights whereas others rely on TD–DFT, but, to our best knowledge, none concerned cyclopentene, dihydrothiophene, or dihydropyrrole structures.^{34,43,55,58–64} The only exception⁶⁵ dealt with the conformers of three cyclopentene-DA species. It is noteworthy that, apart from our previous methodological works,^{34,64} all these TD–DFT investigations have been performed with limited basis sets, 6-31G or 6-31G(d) (or similar), and did not incorporate any modeling of environmental effects. As shown in refs 34 and 64, these small basis sets are not able to provide *theoretically converged* UV/vis data.

This paper is organized as follows: in section II, we describe our computational procedure; in section IIIA, we compare the computed wavelengths with available experimental data; in section IIIB, we establish structure–property relationships; and in section IV, we conclude and provide some insights for future research directions.

II. Methodology

We have chosen the *Gaussian 03*⁶⁶ package of programs to perform the geometry optimizations, vibrational analysis, and excited-state evaluations for the set of DA derivatives drawn in Figure 1. In (TD-)DFT, the choice of the functional is often crucial to yield valuable results. In this contribution, we go for the hybrid PBE0 functional, sometimes refereed to as PBE1PBE.^{67,68} This parameter-free functional is built on the Perdew-Burke-Ernzerhof pure functional,⁶⁹ in which the exchange is weighted (75% DFT/25% HF) according to a theoretical *rationale*;⁷⁰ i.e., absolutely no experimental input as been used to design PBE0.^{67,68} PBE0 has been found successful for cyano and maleic DA,^{34,64} as well as for many other dyes.^{38,71–75} For most organic molecules, the size of the basis set required for an accurate prediction of the ground-state properties is smaller than for the calculation of excited-state energies. As the use of a smaller basis set for geometry optimizations than for TD–DFT calcula-

tions allows a significant gain in cpu time (without loss of accuracy), this procedure has been followed here.

For each system, the ground-state structure has been determined by a standard force-minimization process, and the vibrational spectrum has been systematically determined to⁷⁶ check that all vibrational frequencies are real. These ground-state calculations have been performed with a triple- ζ polarized basis set, 6-311G(d,p), that is known for providing converged ground-state structural parameters for the largest majority of organic molecules,^{77–79} and DA as well.^{34,64} For iodine centers, the well-known LanL2DZ pseudopotential/basis set has been used instead of 6-311G(d,p).

TD–DFT is then used to compute the first three low-lying excited states of DA. As expected from experimental data, the electronic excitation responsible for the color presents a typical $\pi \rightarrow \pi^*$ character associated to a large oscillator force. We have selected the 6-311+G(2d,p) basis set for these TD–DFT calculations, as this basis set has been found adequate and accurate for thioindigo dyes, which possess five-membered sulfur rings in their chromogenic unit as well.⁸⁰ In addition, a further extension of the basis set does not alter the λ_{\max} of DA;^{34,64} i.e., 6-311+G(2d,p) provides *theoretically converged* transition energies ($\Delta E(\text{eV}) = 1239.8424/\lambda_{\max}(\text{nm})$), at least for the low-lying state(s) of interest. As in the first two steps, LanL2DZ pseudopotential/basis set replaces 6-311+G(2d,p) for iodine atoms. The partial atomic charges given in section IIIB have been computed within the Merz–Kollman (MK)^{81,82} and natural population analysis (NPA)⁸³ frameworks using the same basis set(s) as in TD–DFT.

As DA UV/vis spectra are measured in solution, it is essential to include surrounding effects in our simulations.^{71,73,84} Therefore, at each stage, the bulk solvent effects are evaluated by means of the polarizable continuum model (IEF-PCM).⁸⁵ In continuum models, one divides the model into a solute part, the DA derivative, lying inside a cavity, surrounded by the solvent part: cyclohexane (CH), hexane (Hex),⁸⁶ benzene (Benz), dichloromethane (DCM), tetrahydrofuran (THF), methanol (MeOH), or acetonitrile (ACN). To build the cavity, we have used the so-called UA0 radii, but for some geometry optimization for which UAKS radii have been found necessary to obtain converged ground-state geometries. IEF-PCM returns valid solvent effects when no specific interactions link the solute and the solvent molecules. In this paper, we have selected the so-called nonequilibrium procedure for TD–DFT calculations, that has been specifically designed for the study of absorption processes.⁴⁴ Within this procedure, only the electronic distribution of the solvent has time to adapt to the excited state of the solute, whereas the nuclei in the surroundings are frozen.

III. Results and Discussion

A. Comparisons with Experiment. In Tables 1–3, we report theoretical and experimental λ_{\max} for cyclopentene, dihydrothiophene, and dihydropyrrole DA derivatives, respectively. It is worth highlighting that many measurements have been carried out at the photostationary state, and therefore, the deduced λ_{\max} values are not strictly corresponding to the closed-ring form but also partly to the additional peak appearing after irradiation; i.e., practically, the solutions are not open-ring form free.

It turns out that all molecules belong to the C_1 point group, even for the compounds possessing symmetric substitution patterns. Indeed, similarly to the perfluoro derivatives,⁴³ the five-membered bridges we selected here do not present any axial symmetry. By imposing a C_2 symmetry during the geometry

TABLE 1: λ_{\max} (in nm) for the “Cyclopentene” Diarylethene Derivatives (**I** in Figure 1)^a

substitution			λ_{\max}		
R ₁	R ₂	solvent	theo.	exp.	ref
Cl	Cl	Hex	485	444	13,15
Cl	Cl	ACN	479	444	18
Cl	Ph	ACN	535	485	18
CHO	CHO	Benz	670	580	13,15
CHO	CHO	ACN	659	577	18
CH=C(CN) ₂	CH=C(CN) ₂	Benz	865	732	13,15
COOH	COOH	MeOH	599	531	13,15
COOEt	COOEt	ACN	578	540	18
<i>p</i> -Pyr.	<i>p</i> -Pyr.	THF	636	551	21
Ph	Ph	Hex	602	529	13,15
Ph	Ph	CH	603	520	17
Ph	Ph	Benz	605	531	13
Ph	Ph	ACN	595	527	16,18
Ph	<i>p</i> -OMe-Ph	ACN	593	524	18
<i>p</i> -OMe-Ph	<i>p</i> -OMe-Ph	Hex	596	529	13
<i>p</i> -OMe-Ph	<i>p</i> -OMe-Ph	ACN	589	519	16,18
<i>p</i> -CN-Ph	<i>p</i> -CN-Ph	Hex	674	570	13
<i>p</i> -CN-Ph	<i>p</i> -CN-Ph	ACN	677	575	18
<i>p</i> -Cl-Ph	<i>p</i> -Cl-Ph	Hex	615	540	13
<i>p</i> -Br-Ph	<i>p</i> -Br-Ph	Hex	618	539	13
<i>p</i> -Br-Ph	<i>p</i> -Br-Ph	ACN	612	532	18
<i>p</i> -SMe-Ph	<i>p</i> -SMe-Ph	ACN	611	540	18

^a All values with PCM-TD-PBE0/6-311+G(2d,p)//PBE0/6-311G(d,p).

TABLE 2: λ_{\max} (in nm) for the “Dihydrothiophene” Diarylethene Derivatives (**II** in Figure 1)^a

substitution			λ_{\max}		
R ₁	R ₂	R ₃	theo.	exp.	ref
Cl	Cl	H	483	448	22
I	I	H	491	470	23
Cl	CHO	H	589	526	22
CHO	CHO	H	660	582	22
Cl	CH ₂ OH	H	491	452	22
CH ₂ OH	CH ₂ OH	H	482	454	22
Ph	Ph	H	594	524	23
<i>p</i> -OMe-Ph	<i>p</i> -OMe-Ph	H	590	528	23
<i>m</i> -NO ₂ -Ph	<i>m</i> -NO ₂ -Ph	H	640	524	23
thioph.	thioph.	H	614	542	23
benzothiazole	benzothiazole	H	687	598	24
Cl	CHO	CHO	551	512	22

^a All results have been obtained in ACN but for the benzothiazole structure (DCM). See Table 1 for more details.

optimization process, one obtains an unstable DA (one imaginary frequency), although the total energy difference with respect to the stable C₁ form is relatively small. For instance, for **I** with R_{1,2} = Cl (hexane), the C₂ form is less stable by 1.5 kcal/mol than its C₁ counterpart. For the first dihydrothiophene-DA in Table 2, this difference amounts to an almost negligible 0.6 kcal/mol. However, much larger discrepancies are found for the electronic absorption spectra, with the C₂ λ_{\max} being too long by +10 nm (495 instead of 485 nm) in the first case and by +11 nm (494 instead of 483 nm) in the second case. Therefore, all calculations presented below have been performed within the correct C₁ point group. For **I** with CHO side groups, we found that the structure with the oxygen atoms placed on the same side as sulfur atoms is more stable by 4.0 kcal/mol than the conformer with an anti-symmetry. This can be compared to the 1.4 kcal/mol value obtained at the B3LYP/DZVP level:⁶⁵ solvent effects obviously tune the relative stabilities.

As can be seen in Tables 1–3, the auxochromic effect is often well-reproduced by theory, although its amplitude tends to be slightly overestimated. For instance, in acetonitrile, replacing

TABLE 3: λ_{\max} (in nm) for the “Dihydropyrrole” Diarylethene Derivatives (**III** in Figure 1)^a

substitution							λ_{\max}		
pattern	X ₁	X ₂	R ₁	R ₂	R ₃	solvent	theo.	exp.	ref
III-a	S	S	Me	Me	Ph	CH	486	448	26
	S	S	Me	Me	Ph	ACN	480	446	26
	S	S	Me	Me	<i>p</i> -Cl-Ph	CH	487	448	26
	S	S	Me	Me	<i>p</i> -Cl-Ph	ACN	481	446	26
	S	S	Me	Me	<i>p</i> -Me-Ph	CH	485	448	26
	S	S	Me	Me	<i>p</i> -Me-Ph	ACN	479	444	26
	S	S	Me	Me	<i>p</i> -OMe-Ph	CH	485	450	25,26
	S	S	Me	Me	<i>p</i> -OMe-Ph	ACN	478	446	26
	S	S	Cl	Me	<i>p</i> -OMe-Ph	CH	490	450	25
	S	S	Cl	Cl	<i>p</i> -OMe-Ph	CH	492	496	25
	S	S	Cl	Cl	Naphta.	CH	495	460	27
	S	S	CHO	CHO	<i>p</i> -OMe-Ph	CH	672	583	25
	S	O	Me	Me	<i>p</i> -OMe-Ph	CH	457	424	25
	S	S	Me	Me	CH ₂ -Ph	CH	476	438	26
	S	S	Me	Me	CH ₂ -Ph	ACN	468	436	26
	O	O	Me	Me	Ph	CH	435	408	26
O	O	Me	Me	Ph	ACN	434	406	26	
O	O	Me	Me	<i>p</i> -Cl-Ph	CH	436	408	26	
O	O	Me	Me	<i>p</i> -Cl-Ph	ACN	434	406	26	
O	O	Me	Me	<i>p</i> -OMe-Ph	CH	435	408	26	
O	O	Me	Me	<i>p</i> -OMe-Ph	ACN	432	406	26	
III-b					<i>p</i> -OMe-Ph	CH	483	458	25
III-c					<i>p</i> -OMe-Ph	CH	536	500	25
III-d			Ph	Cl	<i>p</i> -OMe-Ph	CH	496	440	25

^aSee Table 1 for more details.

one (two) Cl atoms by phenyl rings shifts the experimental spectra of **I** by +41 nm (+83 nm); changes satisfactorily estimated by theory: +50 nm (+151 nm). The variations induced by adding *para* groups to aryl-substituted-**I** are also nicely reproduced by TD-DFT, although the ranking is reversed for Br/SMe (actually, the λ_{\max} of these two DA are very close). In the **II** series, calculations also succeed in returning the main substitution effects, and the λ_{\max} scale displays a halogen < phenyl < thiophene < aldehyde < benzothiazole pattern, accordingly to experiment. Nevertheless, as for **I**, the shifts are slightly overshoot: +131 nm instead of +94 nm from chlorine to thiophene, for instance. In this **II** series, the only problematic case originates from the *m*-NO₂-Ph groups, as expected for such a compound presenting both a charge-transfer character and nitro groups in *meta* positions. Indeed, the electronic charge transfer tends to be poorly described by TD-DFT that relies on standard functionals.³⁵ On top of that, the *meta* substitution pattern is known to be equally challenging, even for simple substituted benzenes.⁸⁷ For **III-a**, one can also evaluate the impact of heteroatoms included in the five-membered rings. With all other parameters being constant, going from X₁ = X₂ = O to X₁ = S, X₂ = O (X₁ = X₂ = S) leads to experimental bathochromic shifts of +16 nm (+42 nm) that are accurately given by theory: +22 nm (+50 nm). Likewise, varying the R₃ group from phenyl to *p*-substituted phenyl has almost no effect in both theory and experiment. For few dyes of the **I** and **III-a** series, wavelengths are available in both nonpolar and polar solvents, typically (cyclo)hexane and acetonitrile. In all cases but one, (*p*-CN-Ph-substituted-**I**), one notes a negative solvatochromic effect though the electronic excitation related to the λ_{\max} typically presents a $\pi \rightarrow \pi^*$ character (see below). Note that several maleic derivatives display the opposite behavior.⁸⁸ The actual solvatochromic effect is accurately reproduced by the PCM scheme, even for the *p*-CN-Ph exception (+3 nm instead of +5 nm), though the amplitude of the shift tends to be slightly overestimated by the continuum model. As the PCM approach does not account for specific solute-solvent interactions, this indicates that the negative solvatochromism is (very likely) not

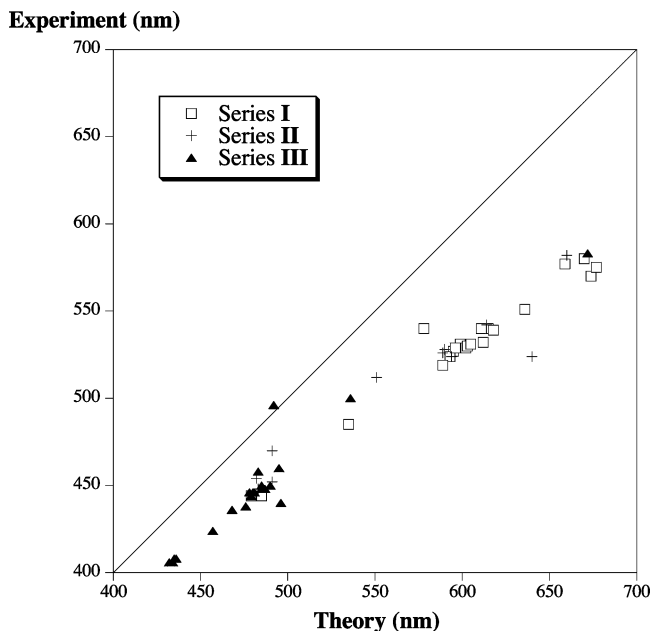


Figure 2. Comparison between raw theoretical and experimental λ_{\max} for DA listed in Tables 1, 2, and 3. All values are in nm. The central line indicates a perfect theory/experiment match. The molecules of series I with $\text{CH}=\text{C}(\text{CN})_2$ side groups has been omitted for clarity.

related to ACN–DA hydrogen bonds. Therefore, this counter-intuitive solvatochromism probably originates in a decrease of the dipole moment upon electronic excitation. Indeed, for **I** with $R_{1,2} = \text{CHO}$, CIS calculations show that the norm of the dipole moment is 0.3 (0.2) debye smaller in the first excited state than in the ground state when a benzene (acetonitrile) environment is considered.

A graphical comparison between theoretical and experimental λ_{\max} is plotted in Figure 2. In all cases (but one, **III-a** with $R_{1,2} = \text{Cl}$ and $R_3 = p\text{-OMe-Ph}$), TD–DFT slightly underestimates the transition energy. However, the experimental value for this dye is subject to caution. Indeed, as can be seen in Table 3, replacing one methyl side group by a chlorine atom gives no shift (0 nm in the experiment, +5 nm in theory), whereas replacing the second methyl group implies a small change with TD–DFT (+2 nm) but leads a strong displacement experimentally (+46 nm): a quite unexpected phenomenon. This mismatch could possibly be related to the nonstandard behavior of this compound.²⁵ Indeed, changing the solvent (from cyclohexane to DCM) impedes any photochromic activity: in DCM irradiation yields a new stable (dehydrogenation) product with completely different absorption spectra.²⁵ The mean absolute errors (MAE) are 74 nm (0.27 eV) for the 22 cases of series **I**, 57 nm (0.24 eV) for the 11 cases of series **II**, and 35 nm (0.20 eV) for the 24 cases of series **III**. The overall MAE, 54 nm (0.23 eV), is significantly larger than for the cyano and maleic derivatives, for which average deviations of 26 nm³⁴ and 9 nm⁶⁴ have been deduced with exactly the same calculation method. Though this 54 nm MAE also exceeds the stand-alone 10 nm (0.05 eV) figure that can be determined for the spectra of the 9 perfluoro-DA simulated by Higashiguchi and co-workers (gas-phase TD–B3LYP/6-31G),⁶¹ such a 0.23 eV MAE is still perfectly in line with the expected TD–DFT accuracy.²⁹ Indeed, considering the studies focused on the valence excited states of dyes or related molecules, one generally observes typical theory/experiment discrepancies close to 0.2–0.3 eV. In fact, we are aware of only 4 studies using a wide panel of organic compounds belonging to several dye families. A couple are due to Fabian and co-workers who reported B3LYP/6-31+G(d)

MAE of 0.29 and 0.24 eV for $\pi \rightarrow \pi^*$ transitions in sulfur-free and sulfur-bearing molecules, respectively;^{41,89} one has been performed by Guillaumont and Nakamura who got B3LYP/6-31G MAE of 0.19 eV for an extended set of dyes,⁴⁰ while the latter by Nguyen and co-workers yields a B3LYP/6-31+G(d) MAE of 0.14 eV for 47 singlet–triplet transitions.⁹⁰ The errors obtained in more specific studies also lie in the same range: from 0.2 to 0.5 eV for coumarins,⁹¹ from 0.3 to 0.4 eV for uranic acid derivatives⁹² or transition-metal complexes,⁹³ and between 0.10 and 0.30 eV for push–pull benzene systems.⁹⁴ Investigations reporting significantly smaller deviations are generally focused on localized transitions, typically belonging to the $n \rightarrow \pi^*$ category.^{41,89,95,96}

With regard to Figure 2, it is striking that, the larger the λ_{\max} , the stronger the TD–DFT overestimation. Indeed, in the **I**-DA series (nonpolar media), the errors are +44 nm with $R_{1,2} = \text{Cl}$, +90 nm with $R_{1,2} = \text{CHO}$, and +133 nm with $R_{1,2} = \text{CH} = \text{C}(\text{CN})_2$. This is consistent with the overestimated auxochromic shifts noted above and can also be deduced for the three DA treated in ref 65. This phenomenon can be explained by the increase of the size of the chromophoric unit (see next section). Obviously, a simple linear regression (SLR) could be applied to polish up these “raw” theoretical values. For the whole DA set, we get (in nm)

$$\lambda_{\max}^{\text{SLR}} = 104.12 + 0.7112\lambda_{\max}^{\text{TD-DFT}} \quad (1)$$

This equation has an excellent R^2 (0.97) and gives an MAE limited to 6 nm (0.03 eV), well below the limits required for designing compounds. If one performs a similar statistical treatment with the set of perfluoro-DA from ref 61, one only gets a fair R^2 (0.79) and MAE (10 nm), although the raw TD–DFT values were closer to experiment. This illustrates that accounting for solvent effects and using sufficiently extended basis set allows better statistical quality and definitively leads to a more consistent description of the chemical effects. One can also build specific equations for any of the three series

$$\lambda_{\max}^{\text{SLR-I}} = 94.13 + 0.7259\lambda_{\max}^{\text{TD-DFT}} \quad (2)$$

$$\lambda_{\max}^{\text{SLR-II}} = 152.09 + 0.6288\lambda_{\max}^{\text{TD-DFT}} \quad (3)$$

$$\lambda_{\max}^{\text{SLR-III}} = 77.00 + 0.7679\lambda_{\max}^{\text{TD-DFT}} \quad (4)$$

that provides R^2 of 0.98, 0.91, and 0.93, respectively. The corresponding MAE values are 5 nm (0.02 eV), 9 nm (0.04 eV), and 6 nm (0.03 eV), respectively, illustrating the great performance of our methodology.

In addition to the absorption wavelengths, the absorption intensities might be of interest for practical developments. It is well-known that the ability of TD–DFT to predict accurate oscillator strengths (f) remains highly questionable, especially for open-shell and/or charged systems.^{43,97,98} For DA, the first challenge for assessing the TD–DFT f accuracy is the lack of (consistent) experimental data about molar extinction coefficients (ϵ), and we consider ref 18 to be the most complete experimental study. The experimental ϵ ordering (with $R_1 = R_2$) is $\text{CHO} < \text{Ph} < p\text{-OMe-Ph} < p\text{-SMe-Ph} < \text{COOEt} < p\text{-CN-Ph} < p\text{-Br-Ph}$, whereas on the basis of f , one gets $\text{CHO} \approx \text{COOEt} < \text{Ph} < p\text{-Br-Ph} \approx p\text{-OMe-Ph} < p\text{-CN-Ph} < p\text{-SMe-Ph}$. This illustrates that TD–DFT does not provide the correct classification for absorption intensities, in the present case. It is sometimes acknowledged that CIS f are more consistent than their TD–DFT counterparts. However, in the present case, CIS

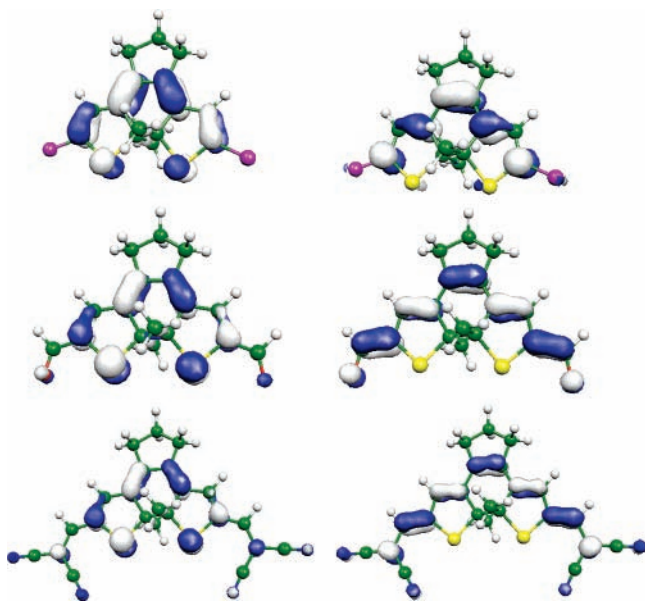


Figure 3. HOMO (left) and LUMO (right) of **I** with $R_{1,2} = \text{Cl}$ (top, Hex), $R_{1,2} = \text{CHO}$ (center, Benz), and $R_{1,2} = \text{CH} = \text{C}(\text{CN})_2$ (bottom, Benz). These plots have been obtained within the PCM–TD–PBE0/6-311+G(2d,p) level of theory.

order is $\text{COOEt} < \text{CHO} < \text{Ph} < p\text{-Br-Ph} \approx p\text{-OMe-Ph} < p\text{-CN-Ph} < p\text{-SMe-Ph}$, and no notable improvement is to be noted (these CIS calculations have been performed on the same geometries, using the same basis sets). Of course, experimental ϵ values are often measured at the photostationary state, which might partly explain the experimental/theoretical discrepancies.

As an intermediate conclusion, we can state that once properly handled the PCM–TD–DFT approach is able to qualitatively reproduce both solvatochromic and auxochromic effects on the λ_{max} , and a quantitative agreement with experiment can straightforwardly be obtained through the use of eq 1. On the contrary, the theoretical oscillator strengths do not model adequately the experimental intensities at this stage of methodological development.

B. Structure–Property Relationships. It is often of great interest to relate the λ_{max} to structural molecular parameters. Before establishing such relationships, it is required to locate the chromophoric unit of DA derivatives. We have used cyclopentene-DA in the following, as they are the most popular among dyes the systems we considered in this work.

For all compounds, the λ_{max} is directly related to a HOMO-to-LUMO transition, and these frontier orbitals have been depicted in Figure 3, for three representative dyes of series **I**. As expected, they are of π nature. It turns out that the HOMO are centered on the sulfur atoms and on the double bonds (see Figure 1) belonging to the five-membered rings and to the central cycle. Contributions from the side groups are very limited, even for the $R_{1,2} = \text{CH} = \text{C}(\text{CN})_2$ -DA. This is in good agreement with the findings of Chen and co-workers for maleic DA.⁶³ As expected, the LUMO implies the central $\text{C}_4\text{--C}'_4$ link as well as the $\text{C}_2\text{--C}_3$ and $\text{C}'_2\text{--C}'_3$ bonds. Therefore, the expected reversal of the double/single pattern upon excitation is confirmed. With chlorine substituents, only the density on the C_1 and C'_1 atoms contributes to the LUMO π -orbital, whereas for the two other molecules in Figure 3 (CHO and $\text{CH} = \text{C}(\text{CN})_2$), both moieties significantly contribute to the LUMO. This illustrates, on one hand, that the chromophoric unit can extend to conjugated side groups, and on the other hand, for the two latter cases, the generated color is associated to a significant charge transfer from the center to the periphery of

the molecule. The first point provides a useful chemical insight for the significant increase of λ_{max} when conjugated side groups are added: the more extended the LUMO, the more stable the excited state, and the smaller the transition energy. The second point clearly explains why TD–DFT absolute error tends to increase for large- λ_{max} -DA (see also Introduction).

The bond length alternation (BLA) is generally regarded as a major geometrical parameter for defining the electron delocalization in π -conjugated molecules.^{99–106} Here, the BLA has been chosen as the (normalized) difference of length between the single and double bond involved in the HOMO (Figure 1)

$$\text{BLA} = \frac{1}{3} (d_{2-3} + d_{2'-3'} + d_{4-4'}) - \frac{1}{4} (d_{1-2} + d_{1'-2'} + d_{3-4} + d_{3'-4'}) \quad (5)$$

For the molecules of series **I**, the BLA are given in Table 4 and vary from 0.047 to 0.091 Å, the former being associated to the $R_{1,2} = \text{Cl}$ molecule and the latter to the $R_{1,2} = \text{CH} = \text{C}(\text{CN})_2$. Therefore, it clearly appears that, the smaller the BLA, the larger the λ_{max} . The R^2 obtained for a linear regression between the BLA and the experimental λ_{max} is 0.95 (the linear correlation between the BLA and the ΔE being a bit weaker ($R^2 = 0.94$)), a nice result, though it, of course, still does not match the accuracy of TD–DFT ($R^2 = 0.98$). Indeed, the BLA is only sensitive to strong auxochromic effects. For instance, DA substituted by two side aryls presents very close BLA (from 0.070 Å (for $p\text{-CN}$) to 0.075 Å (for all others)), although their λ_{max} values slightly differ. Therefore, when using the BLA criterion, the addition of *para*-bromine atoms to the phenyl rings are supposed to have no effect (in ACN), but in reality, the spectrum is shifted by 5 nm. Nevertheless, this study shows that the BLA can be a fast and efficient screening tool for the ordering the λ_{max} of DA derivatives.

To compute the partial atomic charges, we have selected the (average) MK and NPA charges (q) for the atomic centers to which side groups are attached, i.e., carbons 1 and 1'. Indeed, the charges borne by these atoms are presumably the most influenced by auxochroms. These q^{MK} and q^{NPA} are summarized in Table 4. Obviously, there is no easy correlation between these charges and the λ_{max} . For instance, within the NPA framework, Cl and $\text{CH} = \text{C}(\text{CN})_2$ side groups give almost the same q , although they are the two extremes of the λ_{max} possibilities. Actually, the R^2 obtained by linear fitting are extremely small (0.03 for MK and 0.02 for NPA), confirming that these q are not (directly) relevant in the present case. The ground-state dipole moments are more indicative of the absorption wavelengths: the larger $|\vec{\mu}|$, the larger λ_{max} . However, the correlation coefficient is still quite poor ($R^2 = 0.50$), and no quantitative predictions are possible. Indeed, it appears that $|\vec{\mu}|$ is much more sensitive to solvation than λ_{max} .

The energies of both the HOMO and LUMO are given in Table 4. As expected, the LUMO is more sensitive to the substitution pattern than the HOMO, and a low-energy LUMO is related to a large λ_{max} . The linear R^2 between the HOMO–LUMO gap and the experimental ΔE attains 0.97. It is noteworthy that the HOMO–LUMO gap is not a much more efficient indicator of the color of DA derivatives than the BLA. In addition, one can find a linear correlation between the gap and the BLA ($R^2 = 0.94$): the smaller the BLA, the smaller the band gap. Such relationship is typical of conjugated systems and has been unraveled for numerous increasingly long π -conjugated pathways.¹⁰² In ref 18, the authors correlated their electrochemical HOMO–LUMO gap with experimental transi-

TABLE 4: Structural and Energetic Parameters for Molecules Listed Table 1^a

R ₁ , R ₂	solvent	BLA	q ^{MK}	q ^{NPA}	\u0304\u03bc	E ^H	E ^L
Cl	Hex	0.0898	-0.084	-0.220	4.35	-0.192	-0.073
Cl	ACN	0.0913	-0.100	-0.226	5.71	-0.192	-0.072
Cl, Ph	ACN	0.0840	-0.118	-0.194	5.65	-0.187	-0.079
CHO	Benz	0.0710	-0.011	-0.264	10.94	-0.207	-0.117
CHO	ACN	0.0708	-0.004	-0.271	14.30	-0.207	-0.117
CH=C(CN) ₂	Benz	0.0467	-0.026	-0.226	16.73	-0.217	-0.148
COOH	MeOH	0.0775	-0.250	-0.281	10.01	-0.206	-0.107
COOEt	ACN	0.0775	-0.162	-0.286	2.04	-0.202	-0.100
p-Pyr.	THF	0.0738	-0.386	-0.175	7.29	-0.191	-0.098
Ph	Hex	0.0752	-0.235	-0.156	2.95	-0.178	-0.080
Ph	CH	0.0752	-0.241	-0.159	3.59	-0.180	-0.081
Ph	Benz	0.0752	-0.244	-0.157	3.07	-0.179	-0.080
Ph	ACN	0.0744	-0.277	-0.162	4.41	-0.182	-0.083
Ph, p-OMe-Ph	ACN	0.0744	-0.239	-0.159	5.76	-0.179	-0.081
p-OMe-Ph	Hex	0.0735	-0.186	-0.150	4.49	-0.172	-0.073
p-OMe-Ph	ACN	0.0742	-0.214	-0.157	6.22	-0.177	-0.078
p-CN-Ph	Hex	0.0705	-0.273	-0.169	7.90	-0.195	-0.107
p-CN-Ph	ACN	0.0703	-0.299	-0.178	10.25	-0.190	-0.103
p-Cl-Ph	Hex	0.0738	-0.243	-0.159	4.58	-0.183	-0.087
p-Br-Ph	Hex	0.0735	-0.272	-0.160	4.65	-0.184	-0.088
p-Br-Ph	ACN	0.0744	-0.305	-0.166	6.41	-0.184	-0.088
p-SMe-Ph	ACN	0.0742	-0.291	-0.164	7.49	-0.179	-0.082

^a BLA is defined by eq 5(\u00c5), *q* are the average charges on the 1 and 1' carbon atoms (in |*e*|), and |\u0304\u03bc| is the norm of the dipole moment (in debye). E^H and E^L are the energies of the HOMO and LUMO (in au).

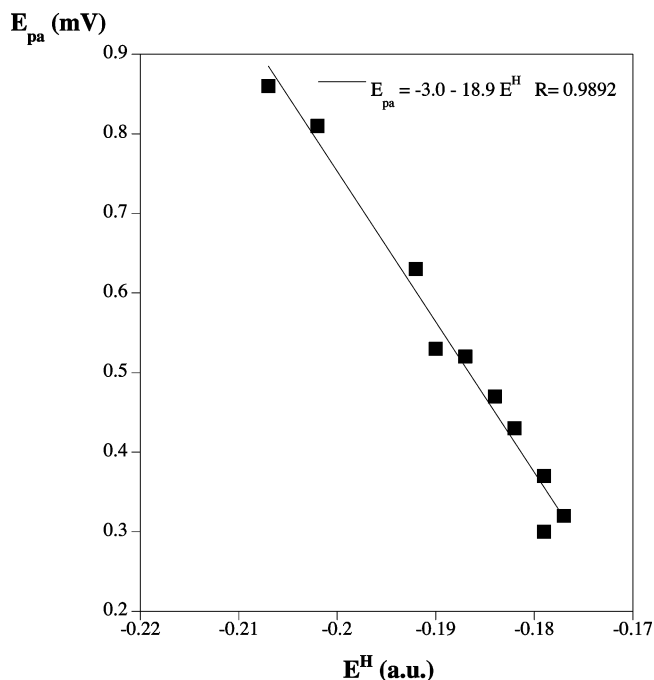


Figure 4. Experimental E_{pa} (ref 18) vs theoretical E^H (HOMO energy). See text for more details.

tion energies and obtained a R^2 of 0.85. In Figure 4, we compare the HOMO energies to the E_{pa} (anionic) energies needed to form (electrochemically) the monocation (10 points, see ref 18). It turns out that they correlate very nicely, showing that the crude Koopmans approximation is valid in this case. There are only six E_{pc} (monoanion formation) values available in ref 18, so statistical comparisons remain difficult.

IV. Conclusions and Outlook

The λ_{max} of closed-ring DA presenting cyclopentene, dihydrothiophene, and dihydropyrrole bridges have been computed using an ab initio TD-PBE0 approach combined with PCM for modeling environmental effects. It turns out that TD-DFT underestimates the transition energies, especially for DA

presenting large λ_{max} . Nevertheless, both auxochromic and solvatochromic displacements are consistently predicted, allowing a quantitative experiment/theory agreement, once a linear correction is set up. Indeed, we obtain a MAE limited to 6 nm or 0.03 eV for the 57 diarylethenes considered. On the contrary, the oscillator strengths computed with TD-DFT are in quite poor agreement with experimental intensities. We have correlated several structural and energetical parameters with the experimental wavelengths, and it turned out that the bond length alternation along the chromophoric path is a very good indicator of the color of DA compounds: the predictive accuracy is sufficient for designing new dyes. Despite its crudeness, the Koopmans approximation allows us to establish a correct ordering for the electrochemical energy required to create cationic DA.

We are currently investigating more precisely the ionization effect on DA derivatives.

Acknowledgment. D.J. and E.A.P. thank the Belgian National Fund for Scientific Research for their research associate positions. The authors thank Prof. J. M. Andr\u00e9 and A. Laurent for their help. All calculations have been performed on the Interuniversity Scientific Computing Facility (ISCF), installed at the Facult\u00e9s Universitaires Notre-Dame de la Paix (Namur, Belgium), for which the authors gratefully acknowledge the financial support of the FNRS-FRFC and the "Loterie Nationale" for the convention number 2.4578.02 and of the FUNDP.

References and Notes

- (1) Irie, M.; Mohri, M. *J. Org. Chem.* **1988**, *53*, 803-808.
- (2) Nakayama, Y.; Hayashi, K.; Irie, M. *J. Org. Chem.* **1990**, *55*, 2592-2596.
- (3) Gilat, S. L.; Kawai, S. H.; Lehn, J. M. *J. Chem. Soc., Chem. Commun.* **1993**, 1439-1442.
- (4) Irie, M.; Sakemura, K.; Okinaka, M.; Uchida, K. *J. Org. Chem.* **1995**, *60*, 8305-8309.
- (5) Gilat, S. L.; Kawai, S. H.; Lehn, J. M. *Chem.-Eur. J.* **1995**, *1*, 275-284.
- (6) Irie, M. *Chem. Rev.* **2000**, *100*, 1685-1716.
- (7) Feringa, B. L. *Molecular switches*; Wiley-VCH: Weinheim, 2001.
- (8) Krayushkin, M. M. *Chem. Heterocycl. Compd. (N. Y., NY, U. S.)* **2001**, *37*, 15-36.

- (9) Dürr, H.; Bouas-Laurent, H. *Photochromism Molecules and Systems*; Elsevier: New York, 2003.
- (10) Matsuda, K.; Irie, M. *J. Photochem. Photobiol., C: Photochem. Rev.* **2004**, *5*, 169–182.
- (11) Tian, H.; Yang, S. *Chem. Soc. Rev.* **2004**, *33*, 85–97.
- (12) Hanazawa, M.; Sumiya, R.; Horikawa, Y.; Irie, M. *J. Chem. Soc., Chem. Commun.* **1992**, 206–207.
- (13) Lucas, L. N. *Dithienylcyclopentene Optical Switches: Towards Photoresponsive Supramolecular Materials*. Ph.D. Thesis, Rijksuniversiteit Groningen, 2001.
- (14) Hania, P. R.; Telesca, R.; Lucas, L. N.; Pugzlys, A.; van Esch, J. H.; Feringa, B. L.; Snijders, J. G.; Duppen, K. *J. Phys. Chem. A* **2002**, *106*, 8498–8507.
- (15) Lucas, L. N.; de Jong, J. J.; van Esch, J. H.; Kellogg, R. M.; Feringa, B. L. *Eur. J. Org. Chem.* **2003**, 155–166.
- (16) Browne, W. R.; de Jong, J. J.; Kudernac, T.; Walko, M.; Lucas, L. N.; Uchida, K.; van Esch, J. H.; Feringa, B. L. *Chem.—Eur. J.* **2005**, *11*, 6414–6429.
- (17) Hania, P. R.; Pugzlys, A.; Lucas, L. N.; de Jong, J. J. D.; Feringa, B. L.; van Esch, J. H.; Jonkman, H. T.; Duppen, K. *J. Phys. Chem. A* **2005**, *109*, 9437–9442.
- (18) Browne, W. R.; de Jong, J. J.; Kudernac, T.; Walko, M.; Lucas, L. N.; Uchida, K.; van Esch, J. H.; Feringa, B. L. *Chem.—Eur. J.* **2005**, *11*, 6430–6441.
- (19) Kudernac, T.; de Jong, J. J. D.; van Esch, J. H.; Feringa, B. L.; Dulic, D.; van der Molen, S. J.; van Wees, B. J. *Mol. Cryst. Liq. Cryst.* **2005**, *430*, 205–210.
- (20) de Jong, J. J.; Browne, W. R.; Walko, M.; Lucas, L. N.; Barrett, L. J.; McGarvey, J. J.; van Esch, J. H.; Feringa, B. L. *Org. Biomol. Chem.* **2006**, *4*, 2387–2392.
- (21) Qin, B.; Yao, R.; Zhao, X.; Tian, H. *Org. Biomol. Chem.* **2003**, *1*, 2187–2191.
- (22) Chen, Y.; Zeng, D. X.; Fan, M. G. *Org. Lett.* **2003**, *5*, 1435–1437.
- (23) Xie, N.; Zeng, D. X.; Chen, Y. *SynLett* **2006**, *5*, 737–740.
- (24) Chen, Y.; Xie, N. *J. Mater. Chem.* **2005**, *15*, 3229–3232.
- (25) Chen, Y.; Zeng, D. X.; Xie, N.; Dang, Y. Z. *J. Org. Chem.* **2005**, *70*, 5001–5005.
- (26) Han, Y.; Zhang, Z. B.; Xiao, J. P.; Yan, W. P.; Fan, M. G. *Chin. Chem. Lett.* **2005**, *16*, 175–178.
- (27) Xie, N.; Chen, Y. *J. Mater. Chem.* **2006**, *16*, 982–985.
- (28) Runge, E.; Gross, E. K. *U. Phys. Rev. Lett.* **1984**, *52*, 997–1000.
- (29) Burke, K.; Werschnik, J.; Gross, E. K. *J. Chem. Phys.* **2005**, *123*, 062206.
- (30) van Caillie, C.; Amos, R. D. *Chem. Phys. Lett.* **1999**, *308*, 249–255.
- (31) van Caillie, C.; Amos, R. D. *Chem. Phys. Lett.* **2000**, *317*, 159–164.
- (32) Furche, F.; Ahlrichs, R. *J. Chem. Phys.* **2002**, *117*, 7433–7447.
- (33) Jacquemin, D.; Perpète, E. A.; Scalmani, G.; Frisch, M. J.; Assfeld, X.; Ciofini, I.; Adamo, C. *J. Chem. Phys.* **2006**, *125*, 164324.
- (34) Jacquemin, D.; Perpète, E. A. *Chem. Phys. Lett.* **2006**, *429*, 147–152.
- (35) Tozer, D. J. *J. Chem. Phys.* **2003**, *119*, 12697–12699.
- (36) Jacquemin, D.; Preat, J.; Perpète, E. A. *Chem. Phys. Lett.* **2005**, *410*, 254–259.
- (37) Jacquemin, D.; Preat, J.; Wathélet, V.; Perpète, E. A. *J. Chem. Phys.* **2006**, *124*, 074104.
- (38) Jacquemin, D.; Preat, J.; Wathélet, V.; Fontaine, M.; Perpète, E. A. *J. Am. Chem. Soc.* **2006**, *128*, 2072–2083.
- (39) Dreuw, A.; Head-Gordon, M. *J. Am. Chem. Soc.* **2004**, *126*, 4007–4016.
- (40) Guillaumont, D.; Nakamura, S. *Dyes Pigm.* **2000**, *46*, 85–92.
- (41) Fabian, J. *Theor. Chem. Acc.* **2001**, *106*, 199–217.
- (42) Schreiber, M.; Bub, V.; Fülischer, M. P. *Phys. Chem. Chem. Phys.* **2001**, *3*, 3906–3912.
- (43) Yokojima, S.; Matsuda, K.; Irie, M.; Murakami, A.; Kobayashi, T.; Nakamura, S. *J. Phys. Chem. A* **2006**, *110*, 8137–8143.
- (44) Cossi, M.; Barone, V. *J. Chem. Phys.* **2001**, *115*, 4708–4717.
- (45) Scalmani, G.; Frisch, M. J.; Mennucci, B.; Tomasi, J.; Cammi, R.; Barone, V. *J. Chem. Phys.* **2006**, *124*, 094107.
- (46) Caricato, M.; Mennucci, B.; Tomasi, J.; Ingrosso, F.; Cammi, R.; Corni, S.; Scalmani, G. *J. Chem. Phys.* **2006**, *124*, 124520.
- (47) Nakamura, S.; Irie, M. *J. Org. Chem.* **1988**, *53*, 6136–6138.
- (48) Ern, J.; Benz, A. T.; Martin, H. D.; Mukamel, S.; Schmid, D.; Tretiaks, S.; Tsiper, E.; Kryschi, C. *Chem. Phys.* **1999**, *246*, 115–125.
- (49) Ern, J.; Benz, A. T.; Martin, H. D.; Mukamel, S.; Tretiaks, S.; Tsyganenko, K.; Kuldova, K.; Trommsdorff, H. P.; Kryschi, C. *J. Phys. Chem. A* **2001**, *105*, 1741–1749.
- (50) Guillaumont, D.; Kobayashi, T.; Kanda, K.; Miyasaka, H.; Uchida, K.; Kobatake, S.; Shibata, K.; Nakamura, S.; Irie, M. *J. Phys. Chem. A* **2002**, *106*, 7222–7227.
- (51) Uchida, K.; Guillaumont, D.; Tsuchida, E.; Mochizuki, G.; Irie, M.; Murakami, A.; Nakamura, S. *THEOCHEM* **2002**, *579*, 115–120.
- (52) Asano, Y.; Murakami, A.; Kobayashi, T.; Goldberg, A.; Guillaumont, D.; Yabushita, S.; Irie, M.; Nakamura, S. *J. Am. Chem. Soc.* **2004**, *126*, 12112–12120.
- (53) Liu, Y.; Wang, Q.; Liu, Y.; Yang, X. Z. *Chem. Phys. Lett.* **2003**, *373*, 338–343.
- (54) Asano, Y.; Murakami, A.; Kobayashi, T.; Kobatake, S.; Irie, M.; Yabushita, S.; Nakamura, S. *THEOCHEM* **2003**, *625*, 227–234.
- (55) Goldberg, A.; Murakami, A.; Kanda, K.; Kobayashi, T.; Nakamura, S.; Uejida, K.; Sekiya, H.; Fukaminato, T.; Kawau, T.; Kobatake, S.; Irie, M. *J. Phys. Chem. A* **2003**, *107*, 4982–4988.
- (56) Uchida, K.; Nakamura, S.; Irie, M. *Bull. Chem. Soc. Jpn.* **1992**, *65*, 430–435.
- (57) Krayushkin, M. M.; Martynkin, A. Y.; Chuvylkin, N. D. *Russ. Chem. Bull.* **2001**, *50*, 381–384.
- (58) Majumdar, D.; Lee, H. M.; Kim, J.; Kim, K. S.; Mhin, B. J. *J. Chem. Phys.* **1999**, *111*, 5866–5872.
- (59) Kobatake, S.; Morimoto, M.; Asano, Y.; Murakami, A.; Nakamura, S.; Irie, M. *Chem. Lett.* **2002**, 1224–1225.
- (60) Giraud, M.; Léaustic, A.; Charlot, M. F.; Yu, P.; Césario, M.; Philouze, C.; Pansu, R.; Nakatani, K.; Ishow, E. *New J. Chem.* **2005**, *29*, 439–446.
- (61) Higashiguchi, K.; Matsuda, K.; Asano, A.; Murakami, A.; Nakamura, S.; Irie, M. *Eur. J. Org. Chem.* **2005**, 91–97.
- (62) Clark, A. E. *J. Phys. Chem. A* **2006**, *110*, 3790–3796.
- (63) Chen, D. Z.; Wang, Z.; Zhao, X. *THEOCHEM* **2006**, *774*, 77–81.
- (64) Perpète, E. A.; Jacquemin, D. *J. Photochem. Photobiol., A* **2007**, *187*, 40–44.
- (65) Guirado, G.; Coudret, C.; Hliwa, M.; Launay, J.-P. *J. Phys. Chem. B* **2005**, *109*, 17445–17459.
- (66) Frisch, M. J.; Trucks, G. W.; Schlegel, H. B.; Scuseria, G. E.; Robb, M. A.; Cheeseman, J. R.; Montgomery, J. A., Jr.; Vreven, T.; Kudin, K. N.; Burant, J. C.; Millam, J. M.; Iyengar, S. S.; Tomasi, J.; Barone, V.; Mennucci, B.; Cossi, M.; Scalmani, G.; Rega, N.; Petersson, G. A.; Nakatsuji, H.; Hada, M.; Ehara, M.; Toyota, K.; Fukuda, R.; Hasegawa, J.; Ishida, M.; Nakajima, T.; Honda, Y.; Kitao, O.; Nakai, H.; Klene, M.; Li, X.; Knox, J. E.; Hratchian, H. P.; Cross, J. B.; Bakken, V.; Adamo, C.; Jaramillo, J.; Gomperts, R.; Stratmann, R. E.; Yazyev, O.; Austin, A. J.; Cammi, R.; Pomelli, C.; Ochterski, J. W.; Ayala, P. Y.; Morokuma, K.; Voth, G. A.; Salvador, P.; Dannenberg, J. J.; Zakrzewski, V. G.; Dapprich, S.; Daniels, A. D.; Strain, M. C.; Farkas, O.; Malick, D. K.; Rabuck, A. D.; Raghavachari, K.; Foresman, J. B.; Ortiz, J. V.; Cui, Q.; Baboul, A. G.; Clifford, S.; Cioslowski, J.; Stefanov, B. B.; Liu, G.; Liashenko, A.; Piskorz, P.; Komaromi, I.; Martin, R. L.; Fox, D. J.; Keith, T.; Al-Laham, M. A.; Peng, C. Y.; Nanayakkara, A.; Challacombe, M.; Gill, P. M. W.; Johnson, B.; Chen, W.; Wong, M. W.; Gonzalez, C.; Pople, J. A. *Gaussian 03*, revision C.02; Gaussian, Inc.: Wallingford, CT, 2004.
- (67) Adamo, C.; Barone, V. *J. Chem. Phys.* **1999**, *110*, 6158–6170.
- (68) Ernzerhof, M.; Scuseria, G. E. *J. Chem. Phys.* **1999**, *110*, 5029–5036.
- (69) Perdew, J. P.; Burke, K.; Ernzerhof, M. *Phys. Rev. Lett.* **1996**, *77*, 3865–3868.
- (70) Perdew, J. P.; Ernzerhof, M.; Burke, K. *J. Chem. Phys.* **1996**, *105*, 9982–9985.
- (71) Guillemoles, J.-F.; Barone, V.; Joubert, L.; Adamo, C. *J. Phys. Chem. A* **2002**, *106*, 11354–11360.
- (72) Petit, L.; Adamo, C.; Russo, N. *J. Phys. Chem. B* **2005**, *109*, 12214–12221.
- (73) Quartarolo, A. D.; Russo, N.; Sicilia, E. *Chem.—Eur. J.* **2006**, *12*, 6797–6803.
- (74) Jacquemin, D.; Bouhy, M.; Perpète, E. A. *J. Chem. Phys.* **2006**, *124*, 204321.
- (75) Pezzella, A.; Panzella, L.; Crescenzi, O.; Napolitano, A.; Navaratan, S.; Edge, R.; Land, E.; Barone, V.; d'Ischia, M. *J. Am. Chem. Soc.* **2006**, *128*, 15490–15498.
- (76) Note that vibrational analysis has been performed for each molecule in one solvent, but not in all solvents in order to gain cpu time.
- (77) Adamo, C.; Scuseria, G. E.; Barone, V. *J. Chem. Phys.* **1999**, *111*, 2889–2899.
- (78) Curtiss, L. A.; Raghavachari, K.; Referm, P. C.; Pople, J. A. *Chem. Phys. Lett.* **1997**, *270*, 419–426.
- (79) Barone, V.; Adamo, C. *J. Chem. Phys.* **1996**, *105*, 11007–11019.
- (80) Jacquemin, D.; Preat, J.; Wathélet, V.; Perpète, E. A. *THEOCHEM* **2005**, *731*, 67–72.
- (81) Besler, B. H.; Merz, K. M.; Kollman, P. A. *J. Comput. Chem.* **1990**, *11*, 431–439.
- (82) Sigfridsson, E.; Ryde, U. *J. Comput. Chem.* **1998**, *19*, 377–395.
- (83) Reed, A. E.; Curtiss, L. A.; Weinhold, F. *Chem. Rev.* **1988**, *88*, 899–926.
- (84) Bertolino, C. A.; Ferrari, A. M.; Barolo, C.; Viscardi, G.; Caputo, G.; Coluccia, S. *Chem. Phys.* **2006**, *330*, 52–59.
- (85) Tomasi, J.; Mennucci, B.; Cammi, R. *Chem. Rev.* **2005**, *105*, 2999–3094.

- (86) Heptane, for which the standard parameters have been defined in *Gaussian 03*, has been used instead of hexane for these calculations.
- (87) Dr. V. Wathélet, personal communication.
- (88) Irie, M.; Sayo, K. *J. Phys. Chem.* **1992**, *96*, 7671–7674.
- (89) Fabian, J.; Diaz, L. A.; Seifert, G.; Niehaus, T. *THEOCHEM* **2002**, *594*, 41–53.
- (90) Nguyen, K. A.; Kennel, J.; Pachter, R. *J. Chem. Phys.* **2002**, *117*, 7128–7136.
- (91) Cave, R. J.; Castner, E. W., Jr. *J. Phys. Chem. A* **2002**, *106*, 12117–12123.
- (92) Danielsson, J.; Ulicny, J.; Laaksonen, A. *J. Am. Chem. Soc.* **2001**, *123*, 9817–9821.
- (93) Petit, L.; Maldivi, P.; Adamo, C. *J. Chem. Theory Comput.* **2005**, *1*, 953–962.
- (94) Jamorski-Jödicke, C.; Casida, M. E. *J. Phys. Chem. B* **2004**, *108*, 7132–7141.
- (95) Jacquemin, D.; Perpète, E. A. *Chem. Phys. Lett.* **2006**, *420*, 529–533.
- (96) Jacquemin, D.; Wathélet, V.; Perpète, E. A. *J. Phys. Chem. A* **2006**, *110*, 9145–9152.
- (97) Hirata, S.; Lee, T. J.; Head-Gordon, M. *J. Chem. Phys.* **1999**, *111*, 8904–8912.
- (98) Rinkevicius, Z.; Tunell, I.; Salek, P.; Vahtras, O.; Agren, H. *J. Chem. Phys.* **2003**, *119*, 34–46.
- (99) Bourhill, G.; Brédas, J. L.; Cheng, L. T.; Marder, S. R.; Meyers, F.; Perry, J. W.; Tiemann, B. G. *J. Am. Chem. Soc.* **1994**, *116*, 2619–2620.
- (100) Meyers, F.; Marder, S. R.; Pierce, B. M.; Brédas, J. L. *J. Am. Chem. Soc.* **1994**, *116*, 10703–10714.
- (101) Brédas, J. L. *Adv. Mater.* **1995**, *7*, 263–274.
- (102) Choi, C. H.; Kertesz, M.; Karpfen, A. *J. Chem. Phys.* **1997**, *107*, 6712–6721.
- (103) Pino, R.; Scuseria, G. *J. Chem. Phys.* **2004**, *121*, 8113–8119.
- (104) Jacquemin, D.; Perpète, E. A.; André, J. M. *J. Chem. Phys.* **2004**, *120*, 10317–10327.
- (105) Jacquemin, D. *J. Phys. Chem. A* **2004**, *108*, 9260–9266.
- (106) Perrier, A.; Maurel, F.; Aubard, J. *J. Photochem. Photobiol., A* In press; doi:10.1016/j.jphotochem.2007.01.030.